

Approximate analytic expressions using Stokes model for tokamak polarimetry and their range of validity

Original

Approximate analytic expressions using Stokes model for tokamak polarimetry and their range of validity / Orsitto, F P; Segre, S E; Subba, F. - In: PLASMA PHYSICS AND CONTROLLED FUSION. - ISSN 0741-3335. - 61:5(2019).
[10.1088/1361-6587/ab09c2]

Availability:

This version is available at: 11583/2986767 since: 2024-03-11T13:23:38Z

Publisher:

IOP PUBLISHING LTD

Published

DOI:10.1088/1361-6587/ab09c2

Terms of use:

This article is made available under terms and conditions as specified in the corresponding bibliographic description in the repository

Publisher copyright

IOP postprint/Author's Accepted Manuscript

"This is the accepted manuscript version of an article accepted for publication in PLASMA PHYSICS AND CONTROLLED FUSION. IOP Publishing Ltd is not responsible for any errors or omissions in this version of the manuscript or any version derived from it. The Version of Record is available online at <http://dx.doi.org/10.1088/1361-6587/ab09c2>

(Article begins on next page)

Approximate analytic expressions using Stokes model for tokamak polarimetry and their range of validity.

F P Orsitto¹ and S E Segre and JET Contributors².

¹CREATE Consortium , Universita di Napoli Federico II , Napoli(Italy) and
ENEA Department Fusion and Nuclear Safety , Frascati(Italy)

²See the author list of X. Litaudon et al 2017 Nucl. Fusion 57 102001

Ref FO/SCOD/1.5.1JET/21052018

Abstract

The analysis of the polarimetry measurements has the aim of validating models[1], with a careful attention to the clarification of their limits of application. In this paper a *new approximation method* is introduced, the so-called SCOD (Special Constant Omega Direction), which gives an analytical solution to the polarimetry exact Stokes model equations. The available approximate solutions (including SCOD) of the polarimetry propagation equations are presented, compared and their application limits determined, using a reference tokamak configuration, which is a simplified equilibrium for a circular tokamak. The SCOD approximation is compared successfully to the Stokes model in the context also of equilibria evaluated for two JET discharges. The approximation methods are analytical or very simple mathematical expressions which can be used also in equilibrium codes for their optimization.

1.Introduction and Motivation of the present work

The analysis of the polarimetry measurements with the aim of improving their use inside the equilibrium codes has the aim of producing models[1,4], with a careful attention to the clarification of their limits of application. These models link the polarimetry measurements like the ellipticity, Faraday Rotation and Cotton-Mouton phase shift to the plasma density, plasma temperature and magnetic field components[3-7]. The Stokes model has been demonstrated [4] as useful tool for the interpretation of the polarimetry: in the present paper a review of the approximate polarimetry models is presented with the determination of their limit of applicability. In this context, a *new approximation method* (so far not appeared in the literature) is also introduced the so-called SCOD (Special Constant Omega Direction, see sec.2) which gives an approximate analytical solution to the Stokes model. The approximation methods presented in this paper are analytical or very simple mathematical expressions which can be used also in equilibrium codes for improving their speed.

The fundamental equation of polarimetry on magnetized plasma [1] is

$$\frac{d\vec{s}}{dz} = \vec{Q} \times \vec{s} \quad (1)$$

Hereafter the eq.1 will be referred as Stokes equation, and the probing beam of radiation (which is monochromatic and fully polarized) is propagating along a vertical chord of a tokamak , taken as z-axis. The radiation wavelength λ and frequency $\omega/2\pi$ are here assumed such that the absorption is negligible. The 3-component Stokes vector $\vec{s} = (s_1, s_2, s_3)$ describes the state of polarization of the radiation and is related to two out of four polarization angles ψ (Faraday rotation), χ (ellipticity $\varepsilon = \tan\chi$) , φ (phase shift angle between two components of the output electric field) and α (ratio between two

components of the output electric field) which characterize the polarization ellipse by the following expressions[4]:

$$\begin{aligned}
s_1 &= \cos(2\chi) \cos(2\psi) = \cos(2\alpha) \\
s_2 &= \cos(2\chi) \sin(2\psi) = \sin(2\alpha) \cos(\varphi) \\
s_3 &= \sin(2\chi) = \sin(2\alpha) \sin(\varphi) \\
s_1^2 + s_2^2 + s_3^2 &= 1
\end{aligned} \tag{2}$$

From the equations (2) the relations between the polarization angles ψ, χ, φ and α and the Stokes vector components can be derived :

$$\tan(2\chi) = \frac{s_3}{\sqrt{s_1^2 + s_2^2}} \tag{3.1}$$

$$\tan(2\psi) = \frac{s_2}{s_1} \tag{3.2}$$

$$\tan(\varphi) = \frac{s_3}{s_2} \tag{3.3}$$

$$\tan(2\alpha) = \frac{\sqrt{s_3^2 + s_2^2}}{s_1} \tag{3.4}$$

The vector $\vec{\Omega}$ depends on plasma parameters and when the plasma frequency ω_p and the electron cyclotron frequency ω_c are such that $\omega \gg \omega_p$ and ω_c . The components of $\vec{\Omega}$ are (CGS units)

$$\begin{aligned}
\Omega_1 &= \frac{\omega_p^2}{2c\omega^3} \left(\frac{e}{mc} \right)^2 (B_x^2 - B_y^2) \\
\Omega_2 &= \frac{\omega_p^2}{c\omega^3} \left(\frac{e}{mc} \right)^2 (B_x B_y) \\
\Omega_3 &= \frac{\omega_p^2}{c\omega^2} \left(\frac{e}{mc} \right) B_z
\end{aligned} \tag{4}$$

Where B_x, B_y, B_z are the components of the magnetic field \vec{B} ; e and m are the electron charge and mass ; c is the velocity of light. The system of coordinates is chosen such that B_z is the component of magnetic field along the propagation axis , B_x is the radial component , B_y is the toroidal component . For polarimetry of magnetized plasma, as it will become clear later , a plasma configuration is characterized by the three dimensionless parameters W_1, W_2, W_3 , defined by

$$W_j = \int_{z_0}^{z_1} \Omega_j(z) dz \quad j = 1, 2, 3 \tag{5}$$

Here z_0 is the abscissa where the probing beam enters the plasma and z_1 is the abscissa where it exits from the plasma.

In experiments $\vec{s}(z_0)$ is known and $\vec{s}(z_1)$ is measured. In general the W_j 's are not directly measured, while their knowledge is useful since they can provide *approximate* constraints in the reconstruction of the plasma MHD equilibrium, in conditions where the polarimetry quantities are small. In ref. [2] this problem is discussed and the MHD equilibrium is solved using the Stokes equations. The parameter W_1 can give the line-integral of plasma density: a quantity quite important for plasma control[3].

The present paper derives and discusses approximate analytic expressions relating W_1 and W_3 to $\vec{s}(z_1)$ which allow to determine these quantities with good approximation from measurements of $\vec{s}(z_1)$ or of two out of the four polarimetric angles.

The work presented here considers the case where the probing beam in the tokamak is in the vertical direction, i.e. it is parallel to the symmetry axis of the plasma torus, and the Stokes vector of the beam at the plasma entrance is $\vec{s}(z_0) = (0, 1, 0)$ so that from eq.(3) it follows that $\psi(z_0) = \pi/4$, $\varphi(z_0) = 0$, $\chi(z_0) = 0$, $\alpha(z_0) = \pi/4$. In this case, calling $\Delta\psi = \psi(z) - \psi(z_0) = \psi(z) - \pi/4$, and $\Delta\alpha = \alpha - \pi/4$, eqs(3.2) and (3.3) give

$$\tan(2\Delta\psi) \equiv -\frac{1}{\tan(2\psi)} = -\frac{s_1}{s_2} \quad (6)$$

$$\tan(2\Delta\alpha) \equiv -\frac{1}{\tan(2\alpha)} = -\frac{s_1}{\sqrt{1-s_1^2}} \quad (7)$$

The reasons of these choices will become clear later.

We derive two alternative sets of approximate analytical expressions relating W_1 and W_3 to $\vec{s}(z_1)$.

The first set (called SCOD approximation) is derived in section 2 from a magnetic configuration where the vector \vec{Q} has constant direction but its modulus $|\vec{Q}|$ depends on z . It will be shown that this configuration is relevant for tokamak polarimetry with beam propagating in vertical direction.

The second set of approximate expressions (which we call 'decoupled approximation') is derived in section 3 for a general magnetic configuration where the coupling between Faraday and the Cotton-Mouton effects is small and possibly negligible. Finally, in sec.4, we will deserve the term 'linear approximation' to the usual approximate expressions (the Type I approximation in ref.3) obtained in the case $W_j \ll 1$ (small polarimetric effects).

In section 5 we describe a reference tokamak configuration which will be used for numerical integration of eqs.(1) in order to obtain exact values for the correspondence between (W_1, W_3) and $\vec{s}(z_1)$. We compare this exact correspondence (i.e. numerical solution of Stokes eqs.(1)) with that provided by the SCOD approximation and also with that provided by the 'decoupled' and 'linear' approximations. This analysis allows to evaluate the quality of the three approximations and to estimate the ranges in (W_1, W_3) over which the approximations give acceptably small differences with respect to the exact correspondence and hence useful in practice.

In section 6 the various approximations, studied in the sections 2-6 in the context of the so-called 'reference tokamak configuration', are tested using an equilibrium evaluated for two JET discharges.

In section 7 the conclusions and future work are outlined.

2.The SCOD(Special Constant Omega Direction) approximation.

It is of interest to consider a particular magnetic configuration for which an exact non-trivial solution to equations (1) exists: this solutions is not yet reported (to our knowledge) in the literature.

This configuration is one where the vector $\vec{\Omega}$ appearing in eqs.(1) has constant direction , i.e. its direction does NOT depend on z. For this **Constant Omega Direction (COD)** approximation we can write

$$\vec{\Omega}(z) = [\Omega_1, \Omega_2, \Omega_3] = \Omega(z) \vec{u} \quad (8)$$

Where $\Omega(z) = \sqrt{\Omega_1^2 + \Omega_2^2 + \Omega_3^2}$ and \vec{u} is a versor whose components u_1, u_2, u_3 , are all constants(i.e. do not depend on z):

$$u_j = \frac{\Omega_j(z)}{\Omega(z)} \quad j = 1, 2, 3 \quad (9)$$

Then calling $W(z) = \int_{z_0}^z \Omega(z) dz$ where $\Omega = |\vec{\Omega}|$ we have

$$W_j(z) \equiv \int_{z_0}^z \Omega_j(z) dz = u_j \int_{z_0}^z \Omega(z) dz = u_j W(z) \quad (10)$$

And so

$$u_j = \frac{W_j(z)}{W(z)} \quad j = 1, 2, 3 \quad (11)$$

For this COD configuration and for the input (initial) Stokes vector $\vec{s}(0) = \vec{s}_0$ the integration of eqs.(1) provides the following expression for $\vec{s}(z)$:

$$\vec{s}(z) = (\vec{s}_0 \cdot \vec{u})\vec{u} + [\vec{s}_0 - (\vec{s}_0 \cdot \vec{u})\vec{u}] \cos W(z) + (\vec{s}_0 \times \vec{u}) \sin W(z) \quad (12)$$

It can be verified that this expression satisfies eqs.(1) when W(z) is given by eq.(10) . The expression (12) is the general solution for the Stokes vector in the COD configuration.

We are interested in the special case where one of the components of $\vec{\Omega}$ (say Ω_2) is zero , so that $\vec{u} = (u_1, 0, u_3)$.

For this **SPECIAL COD (SCOD)** configuration with $\Omega_2 = 0$, we are interested in the case when the input Stokes vector is $\vec{s}(z_0) = (0, 1, 0)$ and then the three components of eq.(12) give :

$$s_1(z) = -u_3 \sin W(z); \quad s_2(z) = \cos W(z); \quad s_3(z) = u_1 \sin W(z) \quad (13)$$

From this point onwards, on all quantities having z dependence , we omit the z dependence to indicate quantities evaluated for $z=z_1$. For example s_1 will indicate $s_1(z_1)$; W will indicate $W(z_1) = \int_{z_0}^{z_1} \Omega(z) dz$ etc...

Now , using eq.(11), the eqs.(13) become:

$$s_1 = -\frac{W_3}{W} \sin W; s_2 = \cos W; s_3 = \frac{W_1}{W} \sin W \quad (14)$$

Where

$$W^2 = W_1^2 + W_3^2 \quad (15)$$

Equations (14) and (15) give the exact correspondence between the output Stokes vector $\vec{s} = (s_1, s_2, s_3)$ and the two quantities W_1 and W_3 for the SCOD configuration when the input Stokes vector is $\vec{s}(z_0) = (0, 1, 0)$.

Of course , this correspondence can be written also in terms of two out of four polarization angles of the output radiation ψ, χ, φ and α instead of s_1, s_2, s_3 . The choice can be made in four different ways , namely (φ, ψ) , (χ, ψ) , (χ, α) , or (φ, α) , which are completely equivalent mathematically as eqs(2) and (3) show. We choose here the couple (φ, ψ) giving the simplest expressions . From eqs(14) and (15) , using eqs (3.2) , (6), and (3.3) we obtain :

$$\tan(2\Delta\psi) = -\frac{s_1}{s_2} = \frac{W_3}{W} \tan W \quad (16)$$

$$\tan \varphi = \frac{s_3}{s_2} = \frac{W_1}{W} \tan W \quad (17)$$

W is given in eq.(15).

This set of equations is entirely equivalent to the set of eqs.(14) and (15) and together provide W_1 and W_3 , ($W_2=0$) of the SCOD configuration as functions of the output Stokes vector or alternatively of the polarimetric angles $\Delta\psi$ and φ .

In this way, calling :

$$P = \tan(2\Delta\psi) = -\frac{s_1}{s_2}; Q = \tan \varphi = \frac{s_3}{s_2} \quad (18)$$

We obtain

$$W_1 = Q \frac{W}{\tan(W)}; W_3 = P \frac{W}{\tan(W)}; W = \arctan(\sqrt{P^2 + Q^2}) \quad (19)$$

Equations (16), (17) and (18), (19) are exact relations for the SCOD configuration.

We will show later that these expressions provide a good approximation for more general configurations in tokamak having vertical beam propagation: so eqs.(19) are approximately valid for these vertical chords.

When we use eqs.(19) as approximate expressions to provide W_1 and W_3 **from the knowledge of the output polarization (s_1, s_2, s_3)** we will call this the SCOD approximation and indicate the values of W_1 and W_3 so obtained by an asterix , W_1^* and W_3^* .

Hence for the SCOD approximation we have :

$$W_1^* = Q [W^*/\tan(W^*)] \quad ; \quad W_3^* = P [W^*/\tan(W^*)] \quad ; \quad W^* = \sqrt{P^2 + Q^2} \quad (20)$$

3.The ‘decoupled’ approximation.

For a general magnetic configuration let us consider the first and third components of eqs.(1):

$$\frac{ds_1(z)}{dz} = \Omega_2(z) s_3(z) - \Omega_3(z) s_2(z) \quad (21)$$

$$\frac{ds_3(z)}{dz} = \Omega_1(z) s_2(z) - \Omega_2(z) s_1(z) \quad (22)$$

Using eqs.(21) and (22) we obtain

$$\frac{d}{dz} \left[\frac{s_3(z)}{s_2(z)} \right] = \Omega_1(z) \left[1 + \left(\frac{s_3(z)}{s_2(z)} \right)^2 \right] - \Omega_2 \frac{s_1(z)}{s_2(z)} - \Omega_3 \frac{s_1(z)s_3(z)}{s_2^2(z)} \quad (23)$$

Regrouping the terms in eq.(23) we obtain

$$\left\{ \left[1 + \left(\frac{s_3(z)}{s_2(z)} \right)^2 \right]^{-1} \right\} \frac{d}{dz} \left[\frac{s_3(z)}{s_2(z)} \right] = \Omega_1(z) - \Omega_2 \frac{s_1(z)s_2(z)}{1 - s_1^2(z)} - \Omega_3 \frac{s_1(z)s_3(z)}{1 - s_1^2(z)} \quad (24)$$

Using eq.(3.3) we can express the right hand side of eq.(24) in terms of φ :

$$\left\{ \left[1 + \left(\frac{s_3(z)}{s_2(z)} \right)^2 \right]^{-1} \right\} \frac{d}{dz} \left[\frac{s_3(z)}{s_2(z)} \right] = \frac{d}{dz} \arctan \left[\frac{s_3(z)}{s_2(z)} \right] \equiv \frac{d\varphi(z)}{dz} \quad (25)$$

Therefore from eqs.(24) and (25) we get

$$\frac{d}{dz} \varphi(z) = \Omega_1(z) - \Omega_2 \frac{s_1(z)s_2(z)}{1-s_1^2(z)} - \Omega_3 \frac{s_1(z)s_3(z)}{1-s_1^2(z)} \quad (26)$$

Integrating the expression (26) with respect to z between $z=z_0$ and $z=z_1$, and recalling that for $\vec{s}(z_0) = (0,1,0)$ one has $\varphi(z_0)=0$ (see section 1), we find

$$\varphi - W_1 = - \int_{z_0}^{z_1} dz \Omega_2 \frac{s_1(z)s_2(z)}{1-s_1^2(z)} - \int_{z_0}^{z_1} dz \Omega_3 \frac{s_1(z)s_3(z)}{1-s_1^2(z)} \quad (27)$$

When the rhs of eq.(27) is small with respect to W_1 the ‘decoupled approximation’ for the Cotton-Mouton phase shift is obtained

$$\varphi \approx W_1 \quad (28)$$

To obtain the same approximation for the Faraday rotation we again use the eqs(22) and (23) :

$$\frac{d}{dz} \left[\frac{s_2(z)}{s_1(z)} \right] = \Omega_3(z) \left[1 + \left(\frac{s_2(z)}{s_1(z)} \right)^2 \right] - \Omega_1 \frac{s_3(z)}{s_1(z)} - \Omega_3 \frac{s_2(z)s_3(z)}{s_1^2(z)} \quad (29)$$

And so

$$\left\{ \left[1 + \left(\frac{s_2(z)}{s_1(z)} \right)^2 \right]^{-1} \right\} \frac{d}{dz} \left[\frac{s_2(z)}{s_1(z)} \right] = \Omega_3(z) - \Omega_1 \frac{s_3(z)}{1-s_3^2(z)} - \Omega_2 \frac{s_2(z)s_3(z)}{1-s_3^2(z)} \quad (30)$$

And using now eq.(3.2)

$$\left\{ \left[1 + \left(\frac{s_2(z)}{s_1(z)} \right)^2 \right]^{-1} \right\} \frac{d}{dz} \left[\frac{s_2(z)}{s_1(z)} \right] = \frac{d}{dz} \arctan \left[\frac{s_2(z)}{s_1(z)} \right] \equiv \frac{d2\psi(z)}{dz} \quad (31)$$

From eqs.(30) and (31) we get

$$\frac{d}{dz} 2\psi(z) = \Omega_3(z) - \Omega_1 \frac{s_3(z)}{1-s_3^2(z)} - \Omega_2 \frac{s_2(z)s_3(z)}{1-s_3^2(z)} \quad (32)$$

Integrating the expression (32) with respect to z between $z=z_0$ and $z=z_1$, we have

$$\Delta(2\psi) - W_3 = - \int_{z_0}^{z_1} dz \Omega_1 \frac{s_1(z)s_3(z)}{1-s_3^2(z)} - \int_{z_0}^{z_1} dz \Omega_2 \frac{s_2(z)s_3(z)}{1-s_3^2(z)} \quad (33)$$

When the rhs of the eq.(33) is small with respect to W_3 , the ‘decoupled approximation’ for Faraday rotation is obtained

$$\Delta(2\psi) \approx W_3 \quad (34)$$

This approximation describes the case where the effect of coupling between Faraday and Cotton-Mouton effects is small and possibly negligible compared to the Faraday effect itself.

When both approximations (i.e. eqs (28) and (34)) hold we shall call the ‘decoupled ‘ approximation. Values provided by this approximation will be indicated by the symbol 0 and so for the ‘decoupled’ approximation we have

$$\varphi = \arctan \frac{s_3}{s_2} = W_1^0 \quad (35)$$

$$\Delta(2\psi) = 2\psi - \pi / 2 = \arctan\left(-\frac{s_1}{s_2}\right) = W_3^0 \quad (36)$$

Using the eqs. (35),(36) , and the $\vec{s} = (s_1, s_2, s_3)$ obtained by the numerical integration of the Stokes equations (1) we can obtain the ‘decoupled ‘ approximation W_1^0 e W_3^0 .

The coupling of Cotton-Mouton and Faraday rotation was studied in ref.6.

4.The ‘linear ‘ approximation .

The ‘Linear’ approximation is obtained integrating the Stokes equations and supposing that W_1 and $W_3 \ll 1$, in this case as it was demonstrated in [1] the series expansion of the solution to the Stokes equation can be restricted to the first term. The so called Type I solution[4] to the Stokes equations is :

$$s_1 = -W_3 = - \int_{z_0}^{z_1} dz \Omega_3 \equiv -W_3^L \quad (37)$$

$$s_2 \approx 1 \quad (38)$$

$$s_3 = W_1 = \int_{z_0}^{z_1} dz \Omega_1 = W_1^L \quad (39)$$

The linear approximation is obtained from the equations (37) and (39) where at the left hand side the numerical solutions to the Stokes equations are inserted. It is clear that in the limit of small polarimetry effects

$$W_3 = W_3^L \quad (40)$$

$$W_1 = W_1^L$$

The ‘Linear’approximation was studied in ref.4 and 6.

5.Reference tokamak configuration

In the present study, we'd like to perform a general study of the approximations useful for polarimetry, with the aim of determining their limits of application. To this aim a 'Reference Tokamak Configuration'(RTC, see ref.5) is used , for exploring a reasonably wide range of parameters possibly also outside the plasma parameters available in devices presently operating.

In order to obtain exact values of the correspondence between $\vec{s} = (s_1, s_2, s_3)$ (which are the values of the components of the Stokes vector evaluated at the output of plasma, integrating numerically the Stokes equations (1)) and the couple (W_1, W_3) we will consider the very simple RTC. This is a tokamak with circular cross section in the limit of very large aspect ratio : the plasma 'torus' becomes a cylinder of radius a, whose axis is the 'toroidal' direction . We take the orthogonal coordinates (x,y,z) with the y-axis on the axis of the plasma cylinder , i.e. the toroidal direction , the z-axis parallel to the symmetry axis of the 'torus' [5]. The two relevant plasma parameters electron density n and current density \vec{j} are taken to depend only to the normalized radius $r = \sqrt{(x^2 + z^2)}/a^2$ and , since we neglect here paramagnetic and diamagnetic effects , \vec{j} has only the y-component. For our calculations we take the following spatial profiles:

$$n = n_0(1 - r^2) \quad (41)$$

$$j = j_0(1 - r^2) \quad (42)$$

We consider propagation of the probing beam of radiation along a vertical chord having equation x=u (dotted line in fig.3 in ref.5). In this geometry we have the density , current profile and the components of magnetic field components given by the following expressions (in CGS units) :

$$(n(z), j(z)) = (n_0, j_0) \left(1 - \frac{(u^2 + z^2)}{a^2} \right) \quad (43)$$

$$B_x(z) = \frac{2I}{ac} \left(\frac{z}{a} \right) \left[2 - \frac{(u^2 + z^2)}{a^2} \right] \quad (44)$$

$$B_z(z) = \frac{2I}{ac} \left(\frac{u}{a} \right) \left[2 - \frac{(u^2 + z^2)}{a^2} \right] \quad (45)$$

$$B_y = B_r = \text{toroidal magnetic field} \quad (46)$$

In units MKS the ratio $(2/c)$ is replaced by $(\mu_0/2\pi)$.

The vector $\vec{\Omega} = (\Omega_1, \Omega_2, \Omega_3)$ can be evaluated by the following expressions:

$$\Omega_1 = H n(z) [B_x(z)^2 - B_r^2] \quad (47)$$

$$\Omega_2 = H n(z) [2B_x(z)B_r] \quad (48)$$

$$\Omega_3 = H n(z) [B_z(z)] \frac{2\omega e}{mc} \quad (49)$$

The constant H is given by

$$H n = \frac{\omega_p^2}{2c \omega^3} \left(\frac{e}{mc} \right)^2 \quad (50)$$

The expressions for the W_j are :

$$W_j = \int_{z_0}^{z_1} dz \Omega_j, ; z_1 = \sqrt{1 - \left(\frac{u}{a}\right)^2}; z_0 = -z_1 \quad (51)$$

In this (simplified) geometry the expressions for W_j appear in the following forms :

$$-W_1 = J B_T^2 - K I_p^2 \quad (52)$$

$$W_2 = L I_p B_T \quad (53)$$

$$W_3 = M I_p \quad (54)$$

The constants J,K,L,M are dependent only by the peaking indexes of the current and density profiles . In the formulas (52),(53),(54) I_p is the plasma current.

The peaking index is the exponent d of the term $(1-r^d)$ appearing in the profiles of density and plasma current (see formulas (41) and (42) , where $d=2$ has been chosen for density and current spatial profiles).

We are interested in considering a family of plasma magnetic configurations which can be obtained varying the values of I_p and B_T , while maintaining fixed n_0 , λ (wavelength of the input radiation) , u (coordinate along the x-axis of the propagation chord), the density and current peaking indexes.

To evaluate the constants J,K,L,M, we can fix the plasma parameters : i.e. for example we choose $a=1$ (minor radius of torus), aspect ratio $R/a=3$, the peaking indexes $d=2$, $q_5=3$, $u/a=0.3$, the laser wavelength $\lambda=195\text{micron}=195 \cdot 10^{-4}\text{cm}$, $n_0=0.510^{14} \text{cm}^{-3}$. and three couples of toroidal magnetic field and plasma current (B_{Tj}, I_{pj}) , $j=0,1,2$. Correspondingly to these plasma parameters we can evaluate $W_{10j}, W_{20j}, W_{30j}$, using the formula (51) together with (47), (48) ,(49). Choosing the following couples :

$$(B_{T_0}, I_{p_0}) = (3T, 3MA)$$

$$(B_{T_1}, I_{p_0}) = (4T, 3MA)$$

$$(B_{T_2}, I_{p_1}) = (3T, 2MA)$$

We determine the values of $W_{10j}, W_{20j}, W_{30j}$ $j=0,1,2$ using the following formulas :

$$\left\{ \begin{array}{l} -W_{10} = J B_{T_0}^2 - K I_{p_0}^2 \\ W_{20} = L B_{T_0} I_{p_0} \\ W_{30} = M I_{p_0} \end{array} \right\}$$

$$\left\{ \begin{array}{l} -W_{11} = J B_{T_1}^2 - K I_{p_0}^2 \\ W_{21} = L B_{T_1} I_{p_0} \\ W_{31} = M I_{p_0} \end{array} \right\}$$

$$\left\{ \begin{array}{l} -W_{12} = J B_{T_2}^2 - K I_{p_1}^2 \\ W_{22} = L B_{T_2} I_{p_1} \\ W_{32} = M I_{p_1} \end{array} \right\}$$

The values of the coefficients (J,K,M) are calculated by :

$$M = \frac{W_{30}}{Ip_0}$$

$$J = \frac{(-W_{10}) - (-W_{11})}{(B_{T0}^2 - B_{T1}^2)}$$

$$K = \frac{(-W_{10}) - (-W_{12})}{(Ip_0^2 - Ip_1^2)}$$

Since we use cylindrical geometry, $W_{20}=0$ and the value $L=0$, because of the perfect symmetry of the poloidal magnetic field with respect to the equatorial plane. The values of the other constants are : $J=0.0105; K=1.8043e-4; M=0.1198$.

In this way we have built a method to create a correspondence between (W_1, W_3) and (Ip, B_T) , since

$$Ip = \frac{W_3}{M} \quad (55)$$

$$B_T = \frac{1}{\sqrt{J}} \sqrt{-W_1 + \frac{K}{M} W_3^2} \approx \sqrt{\frac{(-W_1)}{J}} \quad (56)$$

$$\frac{K}{M} W_3^2 \ll (-W_1)$$

Once obtained the couple (Ip, B_T) , starting from a couple (W_1, W_3) , we can derive the vector $\vec{Q}(z)$ using the formulas (47),(48),(49) and then solve the Stokes eqs.(1) together with the initial condition $\vec{s}(z_0) = (0, 1, 0)$, obtaining finally the value of $\vec{s} = (s_1, s_2, s_3)$.

Starting from these values (i.e. $\vec{s} = (s_1, s_2, s_3)$) we can build the couples (W_1^*, W_3^*) using eqs.(18) and (19), (W_1^0, W_3^0) using eqs.(35) and (36), and (W_1^L, W_3^L) using eqs.(37) and (39).

The accuracy of the various approximations : i.e. SCOD, 'Decoupled' and 'Linear' can be evaluated determining the following ratios :

$$\Delta W_1^* = \frac{((-W_1^*) - (-W_1))}{(-W_1)}; \Delta W_3^* = \frac{((W_3^*) - (W_3))}{(W_3)} \quad (57)$$

$$\Delta W_1^0 = \frac{((-W_1^0) - (-W_1))}{(-W_1)}; \Delta W_3^0 = \frac{((W_3^0) - (W_3))}{(W_3)} \quad (58)$$

$$\Delta W_1^L = \frac{((-W_1^L) - (-W_1))}{(-W_1)}; \Delta W_3^L = \frac{((W_3^L) - (W_3))}{(W_3)} \quad (59)$$

The fig.1 shows the results of this sensitivity calculations of ΔW_1^* vs $(-W_1)$ and W_3 and the fig.2 ΔW_3^* vs $(-W_1)$ and W_3 . The figs. 1 and 2 detect a **strong cross dependence** of ΔW_1^* upon W_3 and ΔW_3^* vs W_1 ; while ΔW_1^* depends very slowly from W_1 at fixed W_3 ; and ΔW_3^* depends very slowly from W_3 at fixed W_1 . Looking into the fig.1 and 2 we can observe that :

- i) $\Delta W_1^* < 15\%$ in the interval $0 < (-W_1) < 1$ and for any value of $0.2 < W_1 < 1$

- ii) $\Delta W_1^* \sim W_3^2$. in the interval $0 < W_3 < 1$ and for any value of $0.2 < -W_1 < 1$
- iii) $\Delta W_3^* < 20\%$ in the interval $0 < (-W_1) < 1$ and for any value of $0.2 < W_3 < 1$
- iv) $\Delta W_3^* \sim W_1^2$ in the interval $0 < (W_3) < 1$ and for any value of $0 < -W_1 < 0.8$

The fig. 3 shows a summary of these calculations for SCOD approximation: *in practice for values of $(-W_1) < 0.5$ and $W_3 < 0.5$ the SCOD approximation gives an evaluation of W_1 and W_3 within 10% accuracy.*

The fig.4 shows the results of sensitivity calculations for the ‘decoupled’ approximation ΔW_3^0 vs $(-W_1)$ and W_3 and the fig.5 ΔW_1^0 vs $(-W_1)$ and W_3 .

Looking into the figs. 4 and 5 it is noted that :

- i) $\Delta W_1^0 \sim W_3^2 f(W_1)$, $\Delta W_1^0 \leq 10\%$ for $0 < -W_1 < 1$ and $W_3 < 0.7$
- ii) $\Delta W_3^0 \sim W_1^2 f(W_3)$, $\Delta W_3^0 \leq 10\%$ for $0 < -W_1 < 0.4$ and $W_3 < 1$

The figure 6 shows a summary of the sensitivity calculations for ‘Decoupled’ approximation : it seems that using this approximation always the evaluation of W_1 and W_3 is within 10% accuracy.

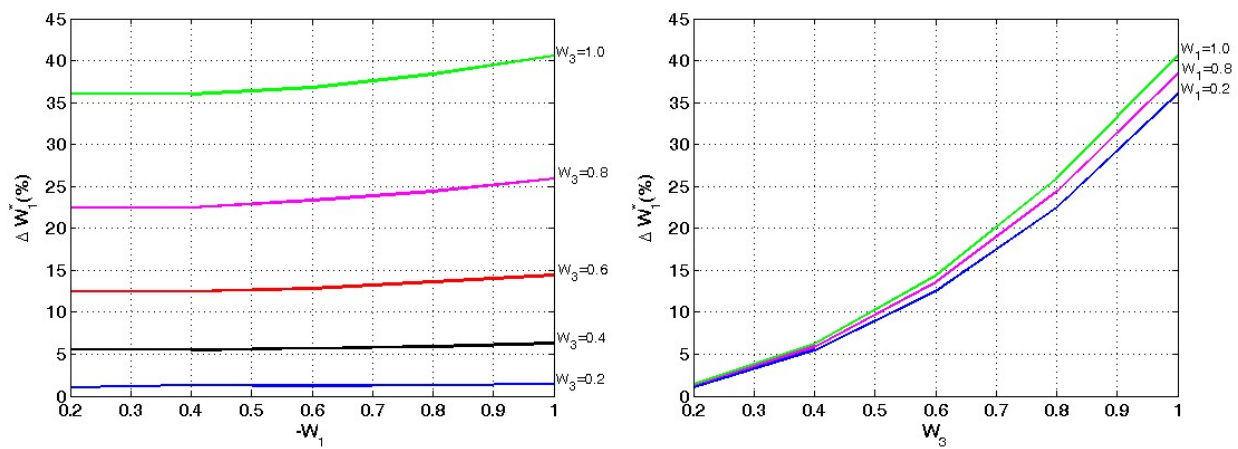


Fig.1. ΔW_1^* vs $(-W_1)$ left figure, and ΔW_1^* vs W_3 right figure.

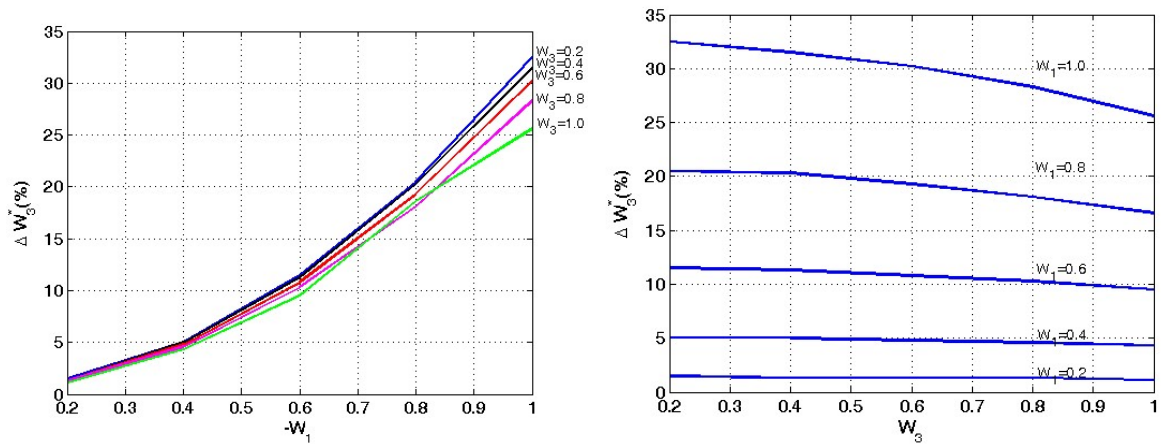


Fig.2. ΔW_3^* vs $(-W_1)$ left figure, and ΔW_3^* vs W_3 right figure.

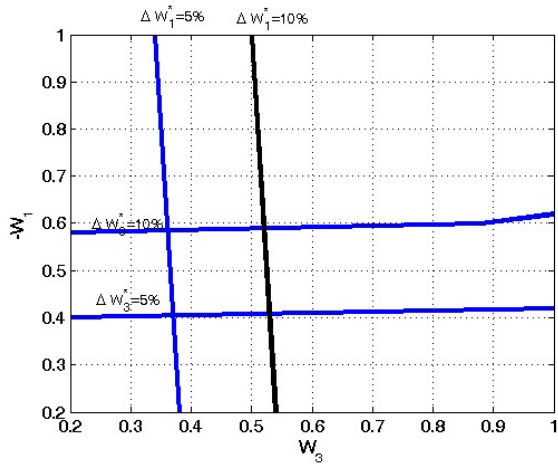


Fig.3. Sensitivity calculations for SCOD approximation.

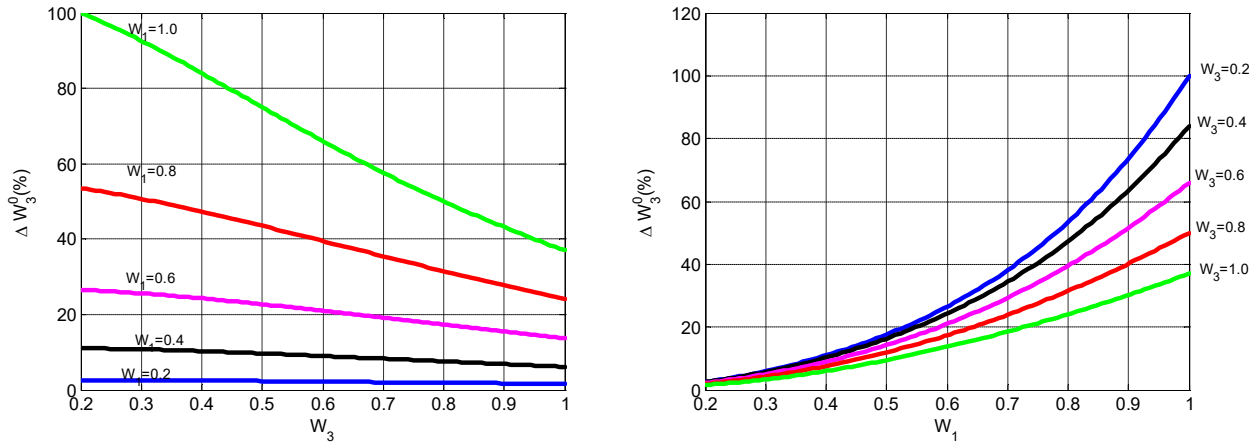


Fig.4. ΔW_3^0 vs W_3 left figure, and ΔW_3^0 vs $(-W_1)$ right figure.

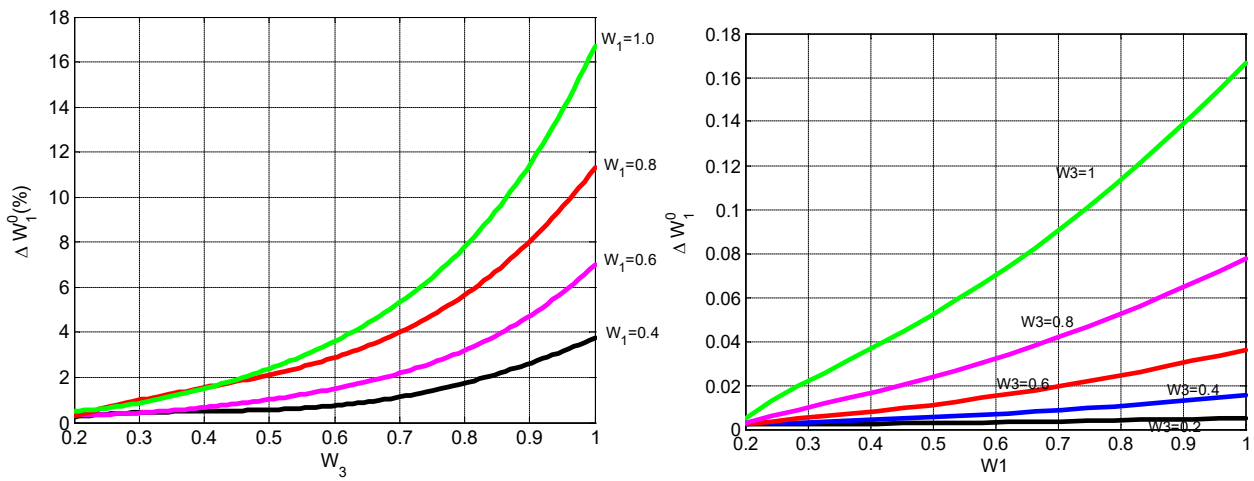


Fig.5. ΔW_1^0 vs W_3 left figure, and ΔW_1^0 vs $(-W_1)$ right figure.

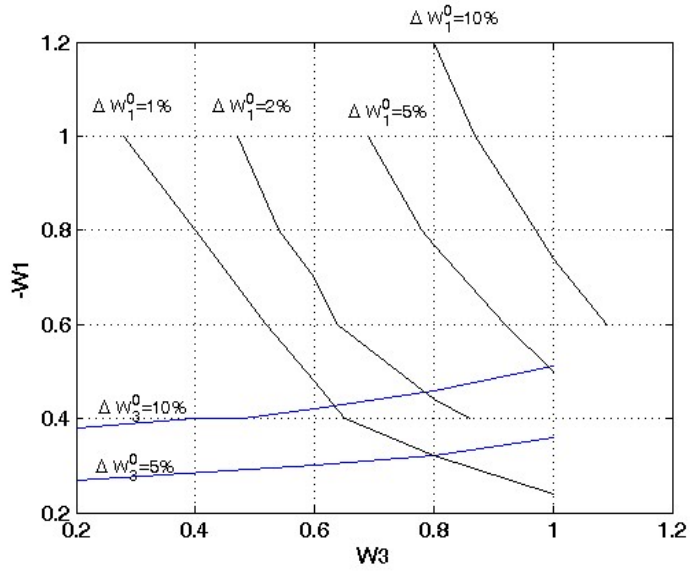


Fig.6. Sensitivity calculations for 'Decoupled' approximation.

6.Sensitivity calculation for a realistic equilibrium : the JET case .

The sensitivity calculations were done in the previous section using analytic equilibrium in circular geometry and slab approximation. These calculations can be considered of limited application, given the conceptual scheme used for the evaluation of the equilibrium .

One can ask whether the same calculations can be done using equilibrium calculated for a real plasma corresponding approximately to the same plasma parameters used for the evaluations shown in figures 1-6.

To give an answer to this question we have selected two JET discharges 92440 and 92441 made in the campaign C36b, the 11th November 2016. The plasma parameters of these discharges are given in Table I.

| JET Pulse # | 92440 | 92441 |
|--|-------|-------|
| $B_T(T)$ | 2 | 3.1 |
| $I_p(MA)$ | 2.1 | 3.5 |
| Line integral density ($10^{19} m^{-2}$) | 16.3 | 21 |

Table I – Plasma parameters of JET pulses used for the sensitivity evaluations using realistic equilibrium.

As it is clear from the plasma parameters these two pulses represent a typical routine pulse (#92440) and an high performance (high magnetic field and current) pulse (#92441). Since these pulses were done subsequently: the machine conditions were approximately the same in these pulses.

The fig.7 shows an example of comparison between Stokes vector calculations for the pulse #92440. Here the calculations are done using the EFTF equilibrium, which is obtained using the polarimetric measurements on the chords #3,5,7 and pressure profiles , as constraints for the equilibrium reconstruction. The values of the components of Stokes vector are evaluated for vertical chords with abscissae in the interval corresponding to major radius $R_0=2.4m -3.7m$, for the time $t=53 s$. In the fig. 7 the blue line connects the points calculated using the numerical integration of the Stokes equations , while the red squares are representatives of the SCOD Approximation. A good agreement is detected between SCOD and the numerical integration of Stokes eqs.

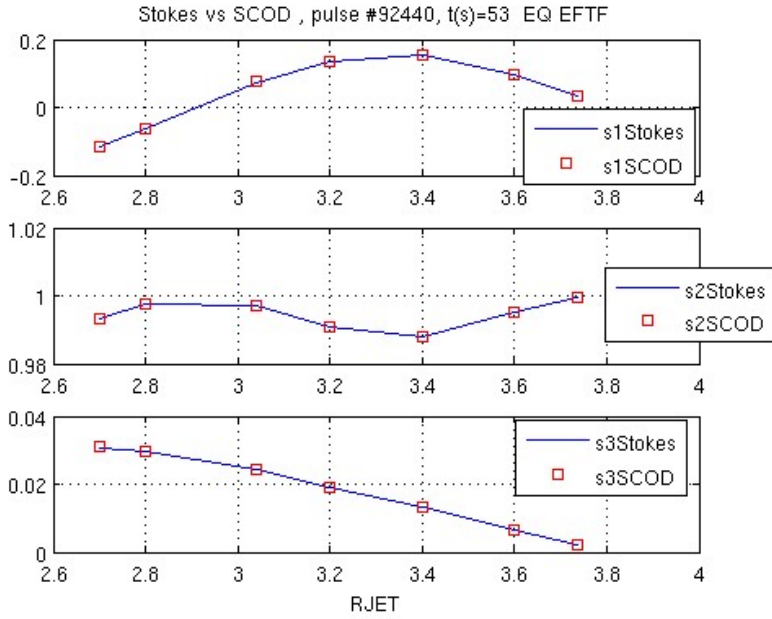


Fig.7.JET Pulse #92440. Comparison of Stokes vector components numerical calculations with SCOD Approximation (SCOD), from the top to bottom s1,s2,s3 respectively : blue line Numerical solution of Stokes eqs.(1), red squares SCOD Approximation.The equilibrium used is EFIT intershot at time t=53s.

Moving to the high performance pulse #92441 the results of the same calculations are shown in fig.8 .

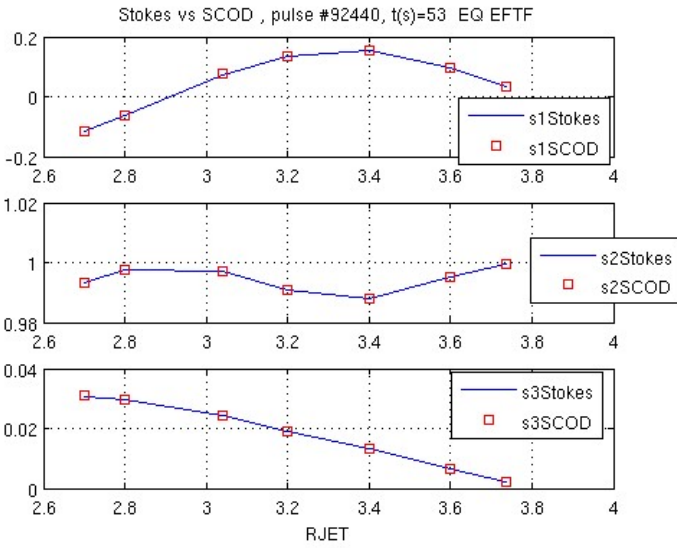


Fig.8. JET Pulse #92441. Comparison of Stokes vector calculations : blue line Numerical solution of Stokes eqs.(1), red squares SCOD Approximation. The equilibrium used is EFTF at time $t=53s$.

The numerical evaluation of the difference between the Stokes and SCOD Approximation is shown in fig.9 for the pulse #92441, where $W_{3Stokes}$ and $W_{1Stokes}$ are defined by the following eqs.

$$W_{3Stokes} = \arctan\left(-\frac{S_1}{S_2}\right) \tag{60}$$

$$W_{1Stokes} = \arctan\left(\frac{S_3}{S_2}\right)$$

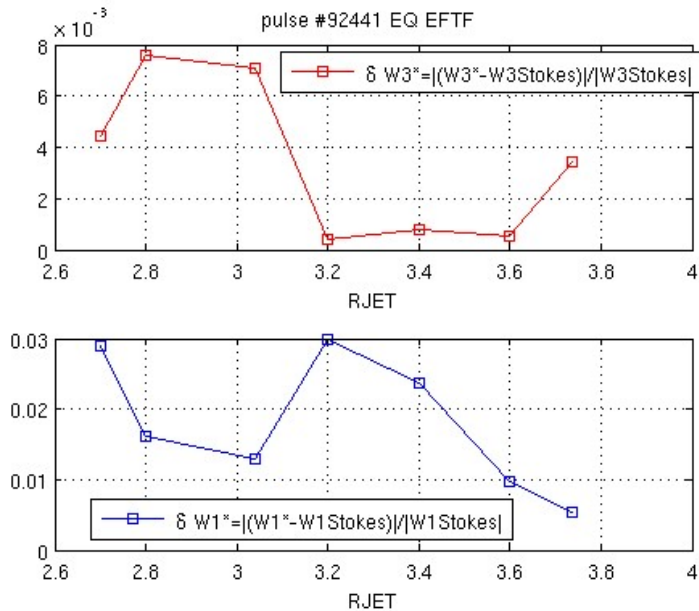


Fig.9 The values of δW_3^* and δW_1^* (defined in the figure) vs the coordinate of the chord along the major radius (RJET).

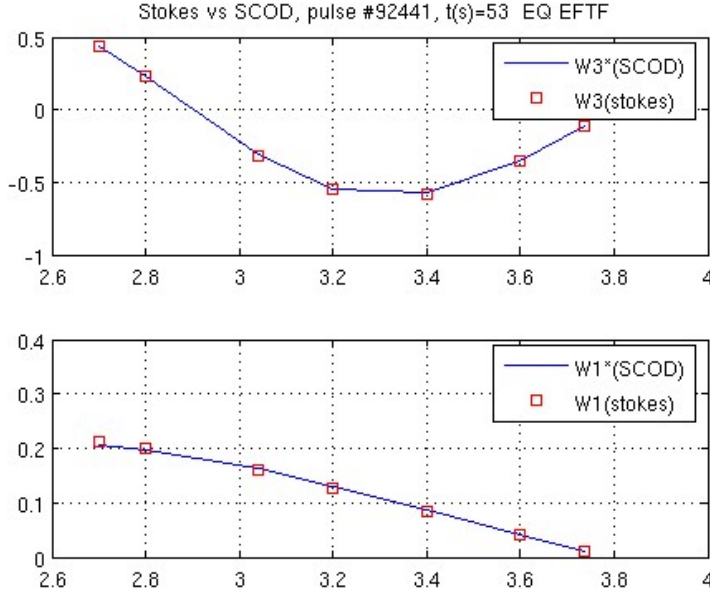


Fig.10. $W_3(\text{Stokes})$ and $W_3^*(\text{SCOD})$, $W_1(\text{Stokes})$ and $W_1^*(\text{SCOD})$, vs the coordinate of the chord along the major radius (RJET).

The figs.9 and 10 give the information that for the pulse #92441 we have $0 < |W_3| < 0.5$ and $W_1 < 0.2$, the error bar using W_3^* instead of $W_{3\text{Stokes}}$ is less than 1%. This is in reasonable agreement with the calculations reported in fig.2(right).

While the error bar on using W_1^* instead of $W_{1\text{Stokes}}$ is less than 3%, for $0 < |W_3| < 1$ and $W_1 < 0.2$: this is in partial agreement with the fig.1(right), where $\Delta W_1^* \leq 10\%$ for $W_3 \leq 0.5$.

The calculations made for the ‘reference tokamak configuration’ used for the calculations shown in fig.1 are pessimistic, since the realistic equilibrium used in the pulse #92441 gives better results in using W_1^* instead $W_{1\text{Stokes}}$.

Given the importance of the Linear approximation in the context of the polarimetry analysis, one can ask about the error bar on using the W_1^L instead of using $W_{i\text{Stokes}}$. The fig.11 shows that for the high performance pulse #92441 this error bar is given by :

$$\delta W_1 = \frac{|W_1^L - W_{1\text{Stokes}}|}{|W_{1\text{Stokes}}|} \leq 7\% \quad ; \quad \delta W_3 = \frac{|W_3^L - W_{3\text{Stokes}}|}{|W_{3\text{Stokes}}|} \leq 6\% \quad (61)$$

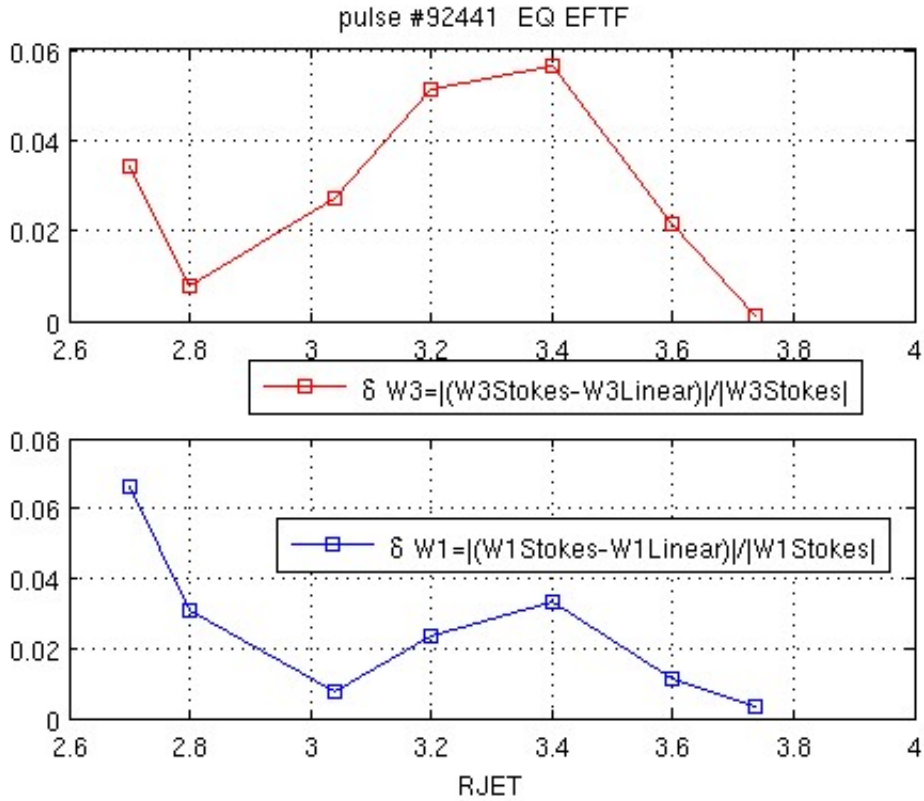


Fig.11. The values of δW_3 and δW_1 (defined in the figure) vs the coordinate of the chord along the major radius (RJET).

The fig.12 shows the same calculations related to the difference of W_1 and W_3 for the decoupled approximation. It turns out that using the decoupled approximation instead of the rigorous solution of the Stokes eqs. Results in error bar of the order of 2% for W_3 and 15% for W_1 .

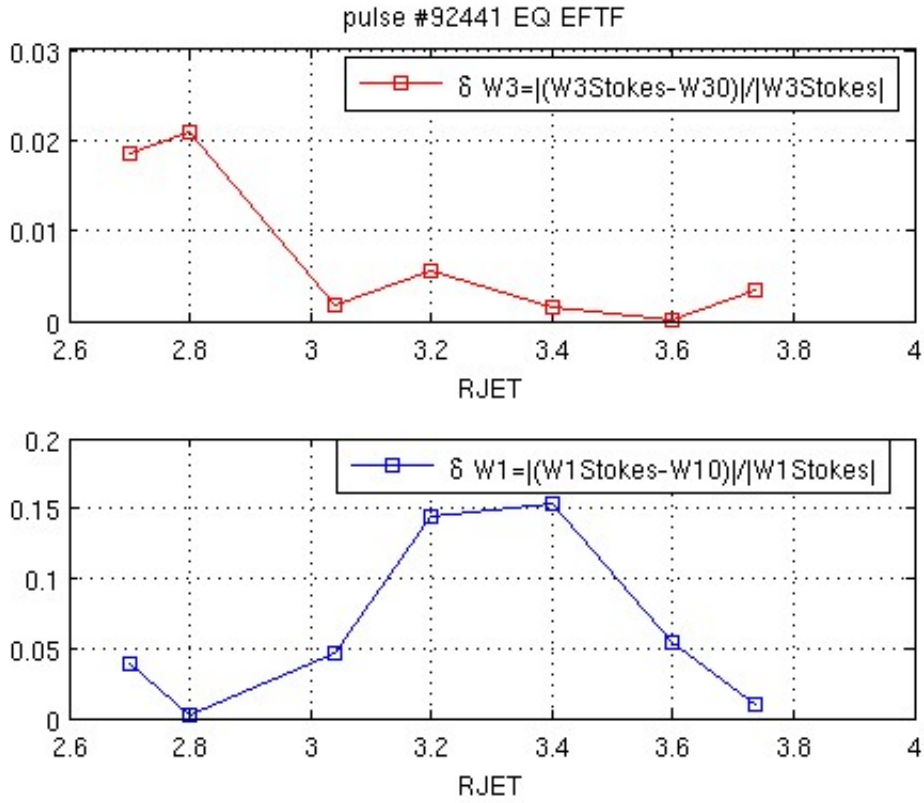


Fig.12. The values of δW_3 and δW_1 vs the coordinate of the chord along the major radius for decoupled approximation (RJET).

7. Conclusions

The analysis of the polarimetry measurements with the aim of improving their use inside the equilibrium codes has the aim of producing models[1,4], with a careful attention to the clarification of their limits of application. In particular simple analytical models (suitably applied) can be useful for the equilibrium code optimization.

In the present paper we present a *new* analytical solution(SCOD, Special Constant Omega Direction) of the Stokes model, which is the reference exact model for propagation of polarized light in plasmas [1,4]. We discuss then SCOD in the context of the analytical approximate models available using a ‘reference tokamak configuration’(RTC) which consists of an equilibrium of a circular tokamak in cylindrical approximation. This study is done to get the general picture of the validity of the models also in range of plasma parameters outside the presently operating tokamak devices . In practice for values of $(-W_1) < 0.5$ and $W_3 < 0.5$ the SCOD approximation gives an evaluation of W_1 and W_3 within 10% accuracy.

These calculations (using RTC) can be considered of limited application, given the conceptual scheme (circular tokamak configuration in cylindrical approximation) used for the evaluation of the equilibrium. One can ask whether the same calculations can be done using equilibrium calculated for a real plasma corresponding approximately to the same plasma parameters used for the evaluations shown in figures 1-6 (obtained using RTC). To give an answer to this question we have selected two JET discharges 92440(Baseline H-mode) and 92441(high performance H-mode). The result is : the error bar using W_3^* (the SCOD equivalent to W_3) instead of $W_{3\text{Stokes}}$ is less than 1%. This is in reasonable agreement with the calculations reported in fig.2(right); while the error bar on using W_1^* (the SCOD equivalent to W_3) instead of $W_{1\text{Stokes}}$ is less than 1% , for $0 < |W_3| < 0.5$ and $W_1 < 0.2$. Given the importance of the Linear approximation (see sec.4) in the context of the polarimetry analysis, one can ask about the error bar on using the W_i^L instead of using $W_{i\text{Stokes}}$: the result is that this error bar is of the order of 6% for the high performance discharge considered. Using the decoupled approximation instead of the rigorous solution of the Stokes eqs. results in error bar of the order of 2% for W_3 and 15% for W_1 .

Acknowledgements

Alexandru Boboc , Blaise Faugeras and David Terranova are gratefully acknowledged for very useful comments. Nick Hawkes is acknowledged for producing the equilibrium calculations used in sec.6.

This work has been carried out within the framework of the EUROfusion Consortium and has received funding from the Euratom research and training programme 2014-2018 under grant agreement No 633053. The views and opinions expressed herein do not necessarily reflect those of the European Commission.

References

- 1.F De Marco and S E Segre , The polarization of an e.m. wave propagating in a plasma with a magnetic shear . The measurement of poloidal magnetic field in a tokamak, Plasma Phys 14(1972)245.
- 2.B Faugeras and F P Orsitto , Equilibrium reconstruction at JET using Stokes model for polarimetry – report RR-9153, INRIA Sophia Antipolis-Mediterranee, 2018 p.1-32.
- 3.A Boboc et al , A novel method for the JET real-time far infrared polarimeter and integration of polarimetry-based line-integrated density measurements for machine protection of a fusion plant – Rev. Sci. Instr. 86(2015)091301
- 4.F Orsitto et al , Modelling polarimetry measurements at JET- Plasma Phys Contr Fusion – **50**(2008)115009; *ibid.* Analysis of Faraday rotation in JET polarimetric measurements – 53 (2011) 035001
- 5.S E Segre , The measurement of poloidal magnetic field in a tokamak by the change of polarization of an electromagnetic wave- Plasma Physics 20(1978)295
- 6.F P Orsitto et al , Mutual Interaction of Faraday rotation and Cotton-Mouton phase shift in JET polarimetric measurements, Rev Sci Instr 81(2010)10D533.
- 7.V V Mirnov et al , Electron kinetic effects on interferometry, polarimetry and Thomson scattering measurements in burning plasmas, Rev Sci Instr 85(2014)11D302